Contents lists available at AccScience Publishing
Nonlinear Scienceand Control Engineering (NSCE)
Vol. 2, No. 1, (2026)
https://accscience.com/journal/nsce

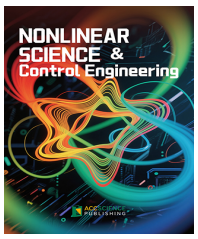

Dynamics and circuit implementation of a memristive chaotic system with switchable equilibrium and multi-parameter amplitude modulation

Ling Wan*

Department of Industrial Automation, Tianyou College, East China Jiaotong University, Nanchang, Jiangxi, China
2023021005000105@ecjtu.edu.cn

History:
Received: January 28, 2026
Revised: April 2, 2026
Accepted: April 8, 2026
Published Online: May 8, 2026

A B S T R A C T

The design and implementation of memristive chaotic systems with switchable equilibria and rich dynamic behaviors have become an important research direction in nonlinear science, owing to their unique potential in engineering applications. In this paper, a non-ideal absolute-value memristor is embedded into a three-dimensional chaotic system (NE_2), constructing a memristive chaotic system (MCS) with multiple types of equilibrium points. By changing the system parameters, the switching between the states with and without equilibrium points can be achieved. This paper analyzes the dynamic characteristics of MCS using bifurcation diagrams, Lyapunov exponents, and phase projections. It discovers that MCS has multi-parameter amplitude modulation and partial mirror symmetry. Meanwhile, under different parameter settings, MCS can generate a wide variety of chaotic and periodic attractors. The reliability of the theoretical analysis is verified through corresponding circuit experiments, and the oscilloscope measurements are highly consistent with the theoretical conclusions, confirming the validity of the constructed chaotic system and laying the foundation for its practical application.

Keywords: Memristive chaotic system; Switchable equilibrium points; Dynamic characteristics; Circuit implementation

1. Introduction

Chaotic systems constitute a crucial research direction in nonlinear science. Characterized by sensitivity to initial conditions and unpredictable long-term behavior, such systems have been widely applied to secure communication, image encryption, and weak-signal detection.[1,2] Currently, one of the mainstream approaches to constructing novel chaotic systems is the modification of classical chaotic systems, which can be roughly divided into two categories: dimension-expanded modification and nonlinear characteristic-enhanced modification. These two approaches improve the dynamic complexity and performance of chaotic systems through distinct paths, and numerous in-depth studies have examined them. Based on classical low-dimensional chaotic systems, dimension-expanded modification alters the original dimensional structure by increasing the system dimension,

*Corresponding author:
Ling Wan (2023021005000105@ecjtu.edu.cn).

Citation:
Ling Wan Dynamics and circuit implementation of a memristive chaotic system with switchable equilibrium and multi-parameter amplitude modulation *Nonlinear Sci Cont Eng*. 2026;2(1):026050003. doi: 10.36922/NSCE026050003

introducing new state variables, or adding feedback functions, enabling low-dimensional systems to exhibit dynamic characteristics they originally lacked by virtue of high-dimensional characteristics.[3] For instance, Pan *et al.*[4] reconstructed a novel chaotic system with extreme multistability by expanding the system dimension and embedding feedback functions. Jie *et al.*[5] extended a self-constructed three-dimensional chaotic system to a four-dimensional one, which exhibited more complex chaotic characteristics after dimension expansion. In contrast, nonlinear characteristic-enhanced modification retains the original dimension of the system. It enhances the system's nonlinear characteristics in the same dimension and reveals richer dynamic behavior by adding nonlinear terms, replacing the original nonlinear functions, or designing new ones.[6] For example, Yang *et al.*[7] introduced a novel nonlinear structure in a three-dimensional framework and constructed a chaotic system with coexisting attractors and an offset boosting effect. Li *et al.*[8] enhanced nonlinearity by optimizing the mapping structure and designed a two-dimensional map with a higher chaotic complexity than the original Logistic map. Zaamoune *et al.*[9] embedded two nonlinear functions into a classical three-dimensional chaotic system, thereby endowing the system with more abundant dynamic characteristics. In summary, these pioneering studies have refined the modification methods of classical chaotic systems through differentiated technical approaches, continuously advanced the research frontier of dynamic behavioral complexity of chaotic systems, and also fully confirmed that designing chaotic systems with rich and intricate dynamic behaviors holds profound theoretical research significance and important engineering application value in the field of nonlinear science and its interdisciplinary research.[10]

The memristor, theoretically predicted by Chua in 1971 and experimentally verified in 2008, is recognized as the fourth fundamental circuit element.[11] Its core characteristic lies in the continuous and non-volatile dynamic change of its resistance value in response to the accumulated charge or magnetic flux passing through it.[12] Leveraging this property, integrating memristors into traditional chaotic systems to construct memristive chaotic systems (MCSs), it is possible to effectively elicit far richer and more complex nonlinear dynamical behaviors that cannot be achieved by traditional chaotic systems alone. For this reason, MCSs have become a research hotspot in nonlinear science in recent years.[13,14] Among various MCSs, equilibrium points have garnered significant attention from scholars in dynamic analysis and engineering applications due to their flexible variability in number and spatial distribution, which often leads to more complex bifurcation paths and richer attractor structures.[15] Fan and Ding[16] constructed an MCS without equilibrium points, revealing its complex chaotic behavior with a maximum Lyapunov exponent (LE) of 1.59, and applied it to highly secure image encryption. He *et al.*[17] incorporated a memristor into a Hopfield neural network (HNN) to construct a memristive two-wing fractional-order HNN model without equilibrium points, simulating neuronal responses to electromagnetic radiation. Kalaichelvi *et al.*[18] proposed a novel chaotic Jerk system with a finite number of equilibrium points and verified its feasibility through circuit implementation. Rahman *et al.*[19] constructed a three-dimensional fractional-order MCS containing only one unstable equilibrium point using a parallel capacitor-inductor structure, which exhibits rich dynamic characteristics. Yu *et al.*[20] built a five-dimensional conservative memristive hyperchaotic system with infinitely many equilibrium points, which shows hyperchaotic and transient quasi-periodic characteristics within a wide parameter range. Wang *et al.*[21] proposed a novel fourth-order MCS with infinitely many unstable equilibrium points and realized the preset-time stabilization of the system using T-S fuzzy modeling and intermittent control strategies. Beyond research on equilibrium points, amplitude modulation, as another core dynamical characteristic that boosts the engineering application potential of MCSs, has also yielded numerous important research advances in this field.[22] Feng *et al.*[23] introduced a novel four-dimensional MCS capable of flexible amplitude and offset control via two independent parameters, providing key technical support for constructing high-performance pseudo-random number generators. Wang *et al.*[24] utilized memristive parameter adjustment to achieve unbounded amplitude modulation and successfully applied it to construct an efficient and highly secure hardware encryption scheme for the Internet of Things. Zhang *et al.*[25] leveraged the synaptic plasticity and electromagnetic radiation effects of memristors to construct a novel dual-memristor-coupled HNN, enabling ultra-large-scale amplitude modulation of various complex chaotic signals and successfully applying it to medical image classification. These relevant studies fully confirm that constructing MCSs with the ability to switch between systems with and without equilibrium points and flexible amplitude modulation holds significant research value in the field of nonlinear systems, and further verify the enormous application potential of such systems in engineering domains, including secure communication, the Internet of Things, and medical image processing.[26,27]

Despite the fruitful existing research, most MCSs suffer from limitations such as a lack of flexible switchability between the states with and without equilibrium points and insufficient multi-parameter amplitude modulation mechanisms, making it difficult to meet the demands of complex scenarios. Addressing the shortcomings of current research, this paper proposes embedding a non-ideal absolute-value memristor into a three-dimensional chaotic system (NE_2) to construct a novel class of MCSs, termed NE_2-MCS. This system exhibits significant performance advantages: flexible and reversible switching between the state with equilibrium points and the state without equilibrium points can be achieved by tuning a single key parameter, enabling the generation of diverse chaotic and periodic attractors, including hidden attractors; mirror symmetry of attractors can be realized simply by reversing the sign of a single parameter. Furthermore, the system possesses unique multi-parameter amplitude modulation and large-scale amplitude modulation. Additionally, this paper validates theoretical analysis through circuit experiments and oscilloscope measurements, confirming the system's strong physical realizability.

2. System description

A general model of the non-ideal magnetically controlled memristor can be expressed as **Equation 1**:

$$\begin{cases} i = W(u)v \\ W(u) = p + q|u| \\ \dot{u} = v - u \end{cases} \tag{1}$$

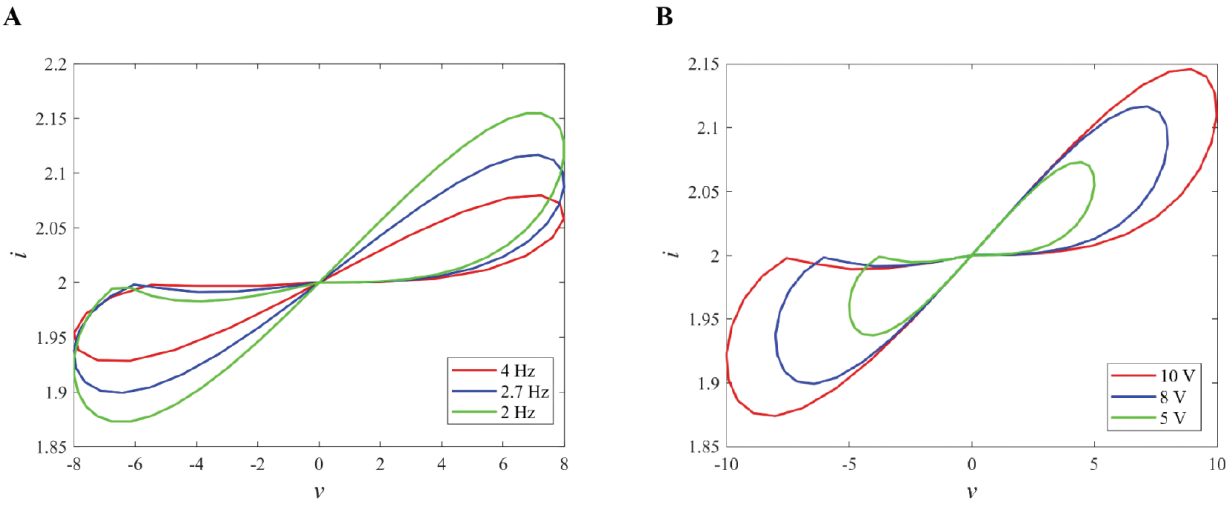

Figure 1. Pinched hysteresis loop of non-ideal absolute-valued memristor with (A) varying frequency and (B) varying amplitude

where p and q are control parameters that regulate the memristor's characteristics, v represents the excitation voltage and i signifies the response current. u and $W(u)$ are the internal magnetic flux and memductance function, respectively. To assess the voltage-current $(v-i)$ characteristics of the model, a sinusoidal voltage stimulus $V = V_m sin(2\pi ft)$ is applied, with the amplitude V_m and frequency f serving as adjustable experimental parameters. For the memristor parameters selected as $p = 1$ and $q = 1$, **Figure 1** shows the $v-i$ characteristic curves under different excitation amplitudes V_m and frequencies f. With the excitation amplitude fixed at $V_m = 8$ V and frequencies set to $f = 2$ Hz, 2.7 Hz, 4 Hz, the lobe area of the hysteresis loop decreases continuously with increasing frequency f, as illustrated in **Figure 1A**. Similarly, when the frequency is fixed at $f = 2.7$ Hz and the amplitude V_m is varied to 5 V, 8 V, and 10 V, the lobe area increases correspondingly with increasing voltage amplitude V_m, as shown in **Figure 1B**. Furthermore, the hysteresis loops of memristor in **Equation 1** exhibit an "8"-shaped profile for different values of f and V_m, which confirms its memory characteristic.

The classical NE_2 system is described in the following differential **Equation 2**:

$$\begin{cases} \dot{x} = -y \\ \dot{y} = x + z \\ \dot{z} = \alpha y^2 + xz - \beta \end{cases} \tag{2}$$

where x, y, and z represent the state variables of the chaotic system, α and β are adjustable control parameters. The system consists of two quadratic nonlinear, three linear, and one constant term. Chaos is observed in the system with $\alpha = 2$ and $\beta = 0.35$. Specifically, the constant term β shifts the system so that the equilibrium condition has no real solution, causing the system to have no equilibrium points. Through the integration of the memristor model (**Equation 1**) into the equation $x = -y$, which corresponds to the first equation of **Equation 2**, a new four-dimensional NE_2-MCS with switchable equilibrium points is established.

The model of the NE_2-MCS can be described as **Equation 3**:

$$\begin{cases} \dot{x} = -(m+n|w|)\cdot y \\ \dot{y} = bx+cz+dy \\ \dot{z} = 4y^2+xz-a \\ \dot{w} = ey-w \end{cases} \tag{3}$$

where w represents the memristive memory dimension, the state variable y acts as the dedicated excitation input to drive the memristor, and the parameters a, b, c, d, e, m, n jointly define the dynamical parameter space. The dissipativity of the NE_2-MCS is defined in **Equation 4**:

$$\nabla V = \frac{\partial \dot{x}}{\partial x} + \frac{\partial \dot{y}}{\partial y} + \frac{\partial \dot{z}}{\partial z} + \frac{\partial \dot{w}}{\partial w} = d + x - 1 \tag{4}$$

with the parameter $a = -1$, $b = 3$, $c = 1.5$, $d = 0.1$, $e = 1$, $m = 2$, $n = 0.2$ and initial values $[-1,\ 1,\ 1,\ 1]$, the NE_2-MCS can generate a strange attractor, as illustrated in **Figure 2**. Substituting the parameter $d = 0.1$ and the initial value $x(0) = -1$ into **Equation 4** satisfies the condition $\nabla V < 0$, which confirms that the system is dissipative.

The LEs serve as indicators of a system's asymptotic stability or instability. Through calculation, the LEs of the attractor generated by the NE_2-MCS are obtained as $LE_1 = 0.2779$, $LE_2 = -0.0005$, $LE_3 = -0.9231$, $LE_4 = -3.3813$. The Lyapunov dimension of the system is shown in **Equation 5**:

$$D = n + \frac{1}{|LE_{n+1}|}\sum_{i=1}^{n} LE_n = 3 - \frac{0.6457}{3.3813} = 2.8090 \tag{5}$$

Let $\dot{x} = \dot{y} = \dot{z} = \dot{w} = 0$ to obtain the set of equilibrium points of NE_2-MCS as **Equation 6**:

$$\begin{aligned} E = \{(x^*,\ y^*,\ z^*,\ w^*)|\ y^* = w^* = 0, \\ x^* = -\tfrac{c}{b}z^*,\ z^* = \pm\sqrt{-\tfrac{b}{c}a}\ \} \end{aligned} \tag{6}$$

Consequently, any equilibrium points $(x^*,\ y^*,\ z^*,\ w^*)$ of NE_2-MCS necessarily satisfy $y^* = w^* = 0$, and it is noteworthy that NE_2-MCS will have different numbers of equilibria by parameters a. The characteristic equation of the NE_2-MCS is shown in **Equation 7**:

$$(1+\lambda)\cdot\left[\lambda^3 + f_1\lambda^2 + f_2\lambda + f_3\right] = 0 \tag{7}$$

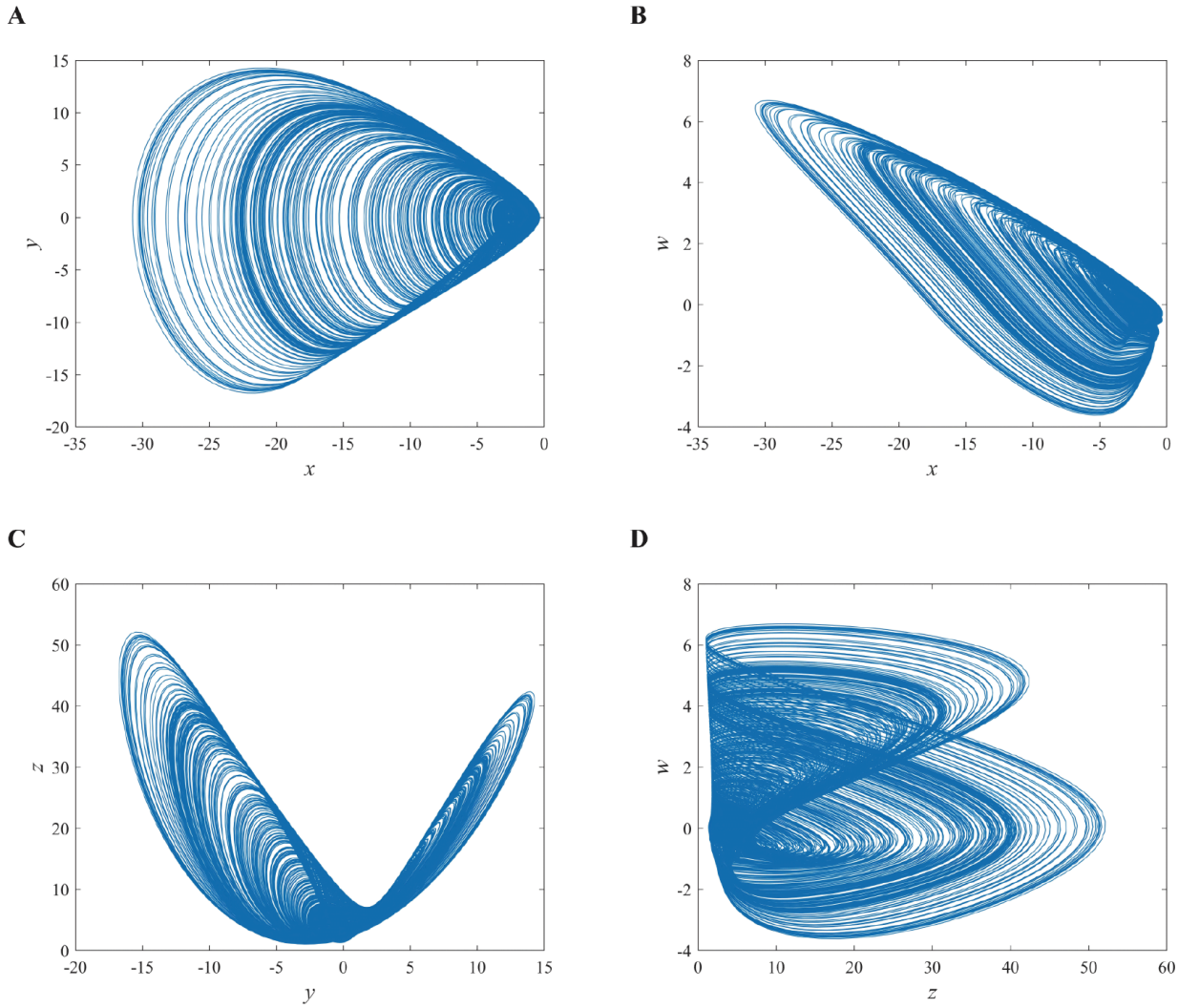

Figure 2. The chaotic behavior of the memristic chaotic system with parameters $a = -1$, $b = 3$, $c = 1.5$, $d = 0.1$, $e = 1$, $m = 2$, $n = 0.2$ and initial values $[-1,\ 1,\ 1,\ 1]$. (A) $x - y$. (B) $x - w$. (C) $y - z$. (D) $z - w$

where $h = (m + n|w|)$, $f_1 = d - \frac{c}{b}$, $f_2 = \frac{cd}{b} - bh$, $f_3 = -ch\left(1 \pm \sqrt{-\frac{b}{c}a}\right)$. Let $a = 0$, then NE_2-MCS has equilibrium points shown in **Equation 5**, especially when $a = 0$, NE_2-MCS has only one equilibrium point $E(0,\ 0,\ 0,\ 0)$. To investigate its stability, we set the parameter $a = -1,\ b = 3,\ c = 1.5,\ d = 0.1,\ e = 1,\ m = 2$, and $n = 0.2$, the corresponding characteristic roots are $\lambda_1 = -1$, $\lambda_2 = 3.0872$, $\lambda_3 = -1.3436 + 0.7353i$, $\lambda_4 = -1.3436 - 0.7353i$ where λ_2 has a positive real part, indicating that E is unstable. When $a > 0$, the NE_2-MCS has no equilibrium point, and under appropriate parameters and initial values, the NE_2-MCS can generate hidden attractors.

3. Dynamics analysis

This section employs various numerical analysis methods, such as LEs, bifurcation diagrams, and phase portraits, to analyze the dynamic characteristics of the proposed chaotic system. It mainly explores parameter-dependent bifurcations, multi-parameter amplitude modulation, and partial mirror symmetry, aiming to uncover the mechanism of its dynamic evolution.

3.1. Diverse bifurcation

For parameters of $a = -1,\ b = 3,\ c = 1.5,\ e = 1,\ m = 2,\ n = 0.2$, and initial values of $[-1,\ 1,\ 1,\ 1]$, NE_2-MCS has equilibrium points. The bifurcation diagram for state variable x and the corresponding LEs obtained by changing d across the interval $[-0.5,\ 0.1]$ are presented in **Figure 3**, which implies that NE_2-MCS approaches chaos through a period-doubling bifurcation sequence as d increases. The corresponding attractor types are summarized in **Table 1**. Evidently, for the parameter values $d = -0.3, -0.2, -0.1$, and 0.1, there are period-1, period-2, period-4, and chaotic attractors, respectively. **Figure 4** shows the $x - y$ plane phase trajectories of the system for different k values.

For parameter values of $a = 1,\ b = 2,\ c = 1.1,\ d = 0.2,\ e = 1$, and $n = 0.2$, with initial values of $[-1,\ 1,\ 1,\ 1]$, NE_2-MCS can generate diverse hidden attractors because it has no equilibrium points. We vary the parameter m within the range ? $[1.9,\ 4.5]$. When $m \in [2.3,\ 2.48]$, the system enters a period-4 state; when $m \in [2.48,\ 3.57]$, the system exhibits a period-2 state; and when $m \in [3.57,\ 4.5]$, the system is in a period-1 state. From the LEs and bifurcation diagram in **Figure 5**, it can be concluded that NE_2-MCS contains hidden attractors at this time, and as m continuously increases, it demonstrates a transition from a

Table 1. Attractors and their corresponding plots for varying d with equilibrium points and for varying m without equilibrium points

Equilibrium-point type	Parameters		Attractors	Figures
With an equilibrium point	d	-0.3	Period-1	Figure 4A
		-0.2	Period-2	Figure 4B
		-0.1	Period-4	Figure 4C
		0.1	Chaos	Figure 4D
Without an equilibrium point	m	2.0	Chaos	Figure 6A
		2.4	Period-4	Figure 6B
		3.0	Period-2	Figure 6C
		4.0	Period-1	Figure 6D

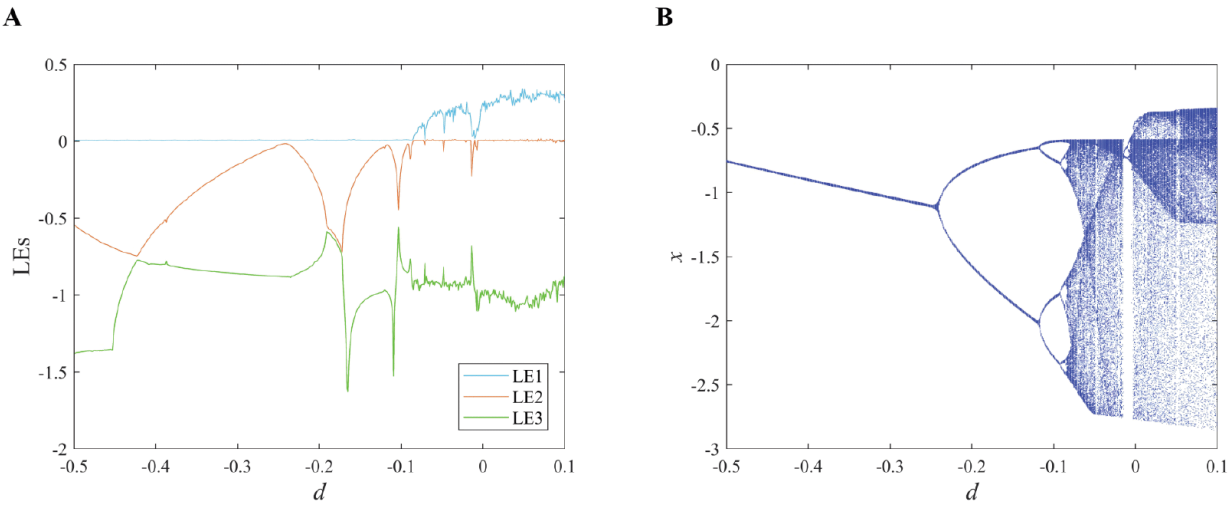

Figure 3. Memristive chaotic system with $a = -1, b = 3, c = 1.5, e = 1, m = 2, n = 0.2$, and $d \in [-0.6,\ 0.1]$. (A) Lyapunov exponents (LEs). (B) Bifurcation diagram.

chaotic state to a gradually stabilizing periodic orbit through period-doubling bifurcations. Similarly, several different values of m are selected and listed in **Table 1**, with the corresponding phase projections on the $x - y$ plane depicted in **Figure 6**.

3.2. Rich signal control

In MCS, amplitude modulation of parameters is mainly used to regulate the system's dynamical behavior. Specifically, it can change the shape, size, and complexity of chaotic attractors and induce bifurcations and chaotic behavior. For the purpose of exploring the chaotic amplitude modulation characteristics of the NE_2-MCS, parameter a is designated as the control variable, with the system parameters set to $b = 3$, $c = 1.5$, $d = 0.1$, $e = 1$, $m = 2$, $n = 0.2$, and the initial values configured as $[-1,\ 1,\ 1,\ 1]$. We take $a = -0.1,\ -1,\ -10,\ -20$, the phase projection diagrams on the $z - w$ plane and the time series diagrams of the state variable z are plotted, and the corresponding results are shown in **Figure 7**. It can be seen from the amplitude modulation phenomenon reflected in the diagrams that the amplitude of the NE_2-MCS is positively correlated with the value of parameter a, which implies that the scale of the attractor increases progressively with the increase of parameter a. Notably, other parameters in the system also exhibit small-scale chaotic amplitude modulation characteristics analogous to those of a, and thus, the simulation results of the amplitude modulation characteristics for the rest of the parameters are not presented separately herein.

Furthermore, in addition to small-scale chaotic amplitude modulation under multi-parameter regulation, the system also demonstrates large-scale chaotic amplitude modulation. With the parameters set as $a = 1, c = 1.1, d = 0.2, e = 1, m = 2, n = 0.2$, and the initial values configured as $[-1,\ 1,\ 1,\ 1]$, **Figure 8** presents the time series plots and local $x - y$ phase portraits of the system with respect to the variation of control parameter b over the range of $[2,\ 100]$. The graphical analysis reveals a positive correlation between the amplitude of the system's chaotic attractors and the parameter b, enabling large-scale amplitude modulation. Interestingly, the morphology of the attractor changes with increasing b. When b is small, NE_2-MCS features a large attractor; as b increases, the attractor shrinks; once b surpasses the critical value of 2.5 and continues to grow, the attractor's size expands again. This change process is illustrated in **Figure 8B**. It indicates that the system may exhibit distinct dynamic modes across parameter intervals, and changes in attractor size reflect the system's switching between modes.

To investigate the periodic amplitude modulation of the system, we set $a = 1, b = 2, c = 1.1, d = 0.2, e = 1, n = 0.2$, and the initial values configured as $[-1,\ 1,\ 1,\ 1]$. Then, we take $m = 3.7,\ 4.1,\ 4.5,\ 4.8$ and plot the projections of the system's chaotic attractors on the $x - y$ and $x - w$ plane in **Figure 9**. It can be observed from the figures that as the parameter m increases, the periodic attractors also enlarge, and the attractors on $x - w$ plane shift accordingly.

Partial mirror symmetry is a form of restricted symmetry in which a dynamical system exhibits mirror-reflection invariance only in a low-dimensional

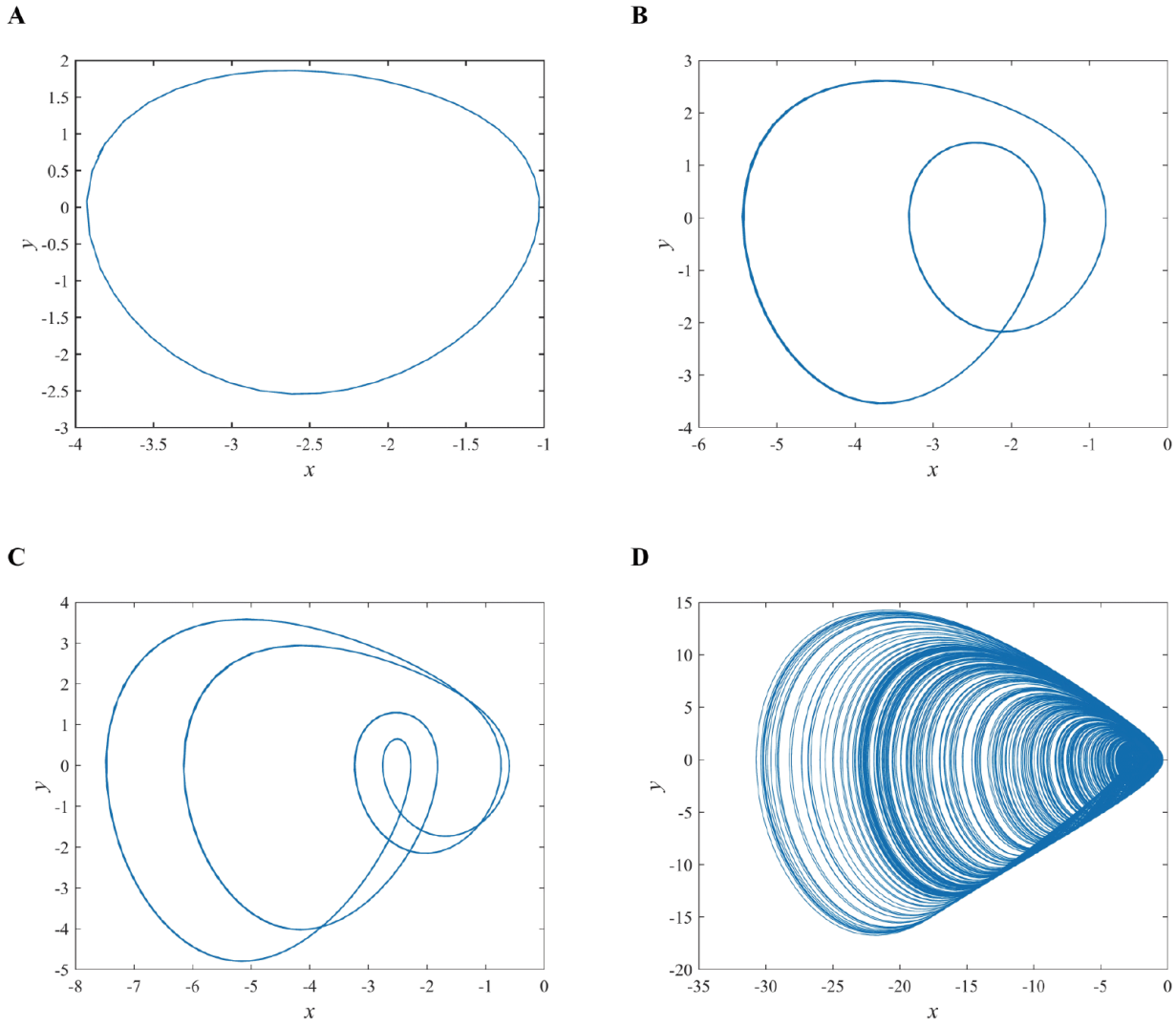

Figure 4. Different attractors of the memristive chaotic system with $a = -1$, $b = 3$, $c = 1.5$, $e = 1$, $m = 2$, $n = 0.2$, and $d \in [-0.6,\ 0.1]$. (A) Period for $d = -0.3$. (B) Period for $d = -0.2$. (C) Period for $d = -0.1$. (D) Chaos for $d = 0.1$

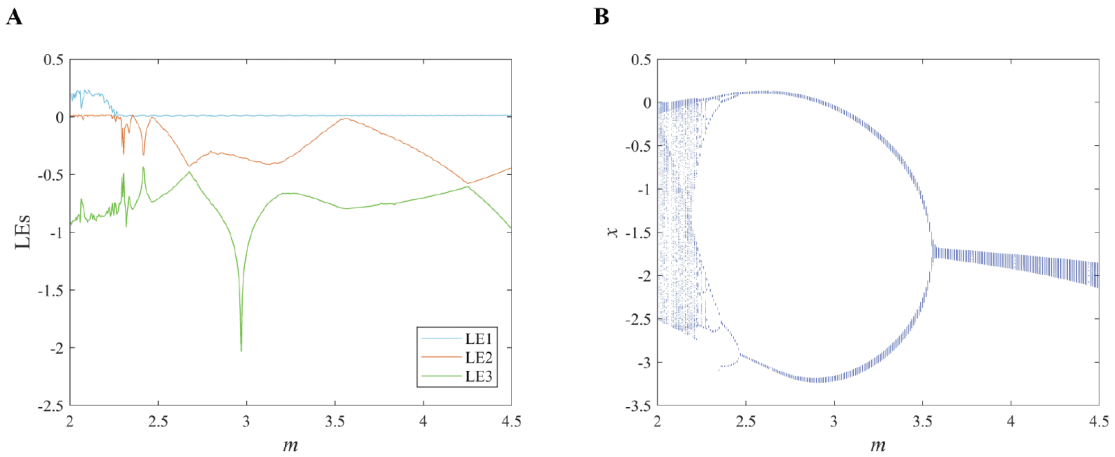

Figure 5. Memristive chaotic system with $a = 1$, $b = 2$, $c = 1.1$, $d = 0.2$, $e = 1$, $n = 0.2$ and $m \in [1.9,\ 4.5]$. (A) Lyapunov exponents (Les). (B) Bifurcation diagram

subspace of the full phase space, while the remaining dimensions remain asymmetric. In NE_2-MCS, partial mirror symmetry can be induced in a four-dimensional phase space by simply reversing the sign of a single parameter d: trajectories within the $(x,\ w)$ and $(z,\ w)$ subplanes display approximate mirror symmetry, while the remaining coordinates remain unchanged. However, no corresponding relationship is observed in the

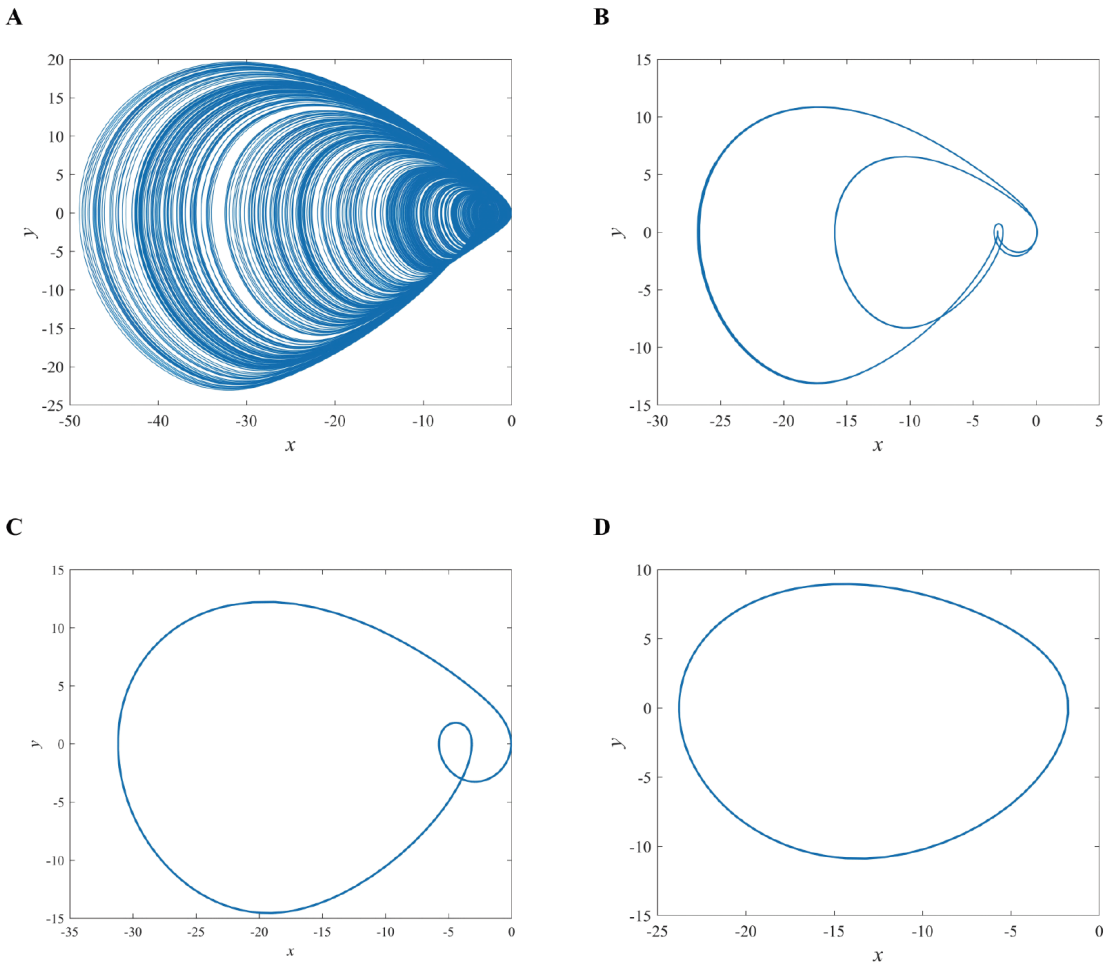

Figure 6. Different attractors of the memristive chaotic system with $a = 1$, $b = 2$, $c = 1.1$, $d = 0.2$, $e = 1$, $n = 0.2$ and $m \in [1.9,\ 4.5]$. (A) Chaos for $m = 2$. (B) Period for $m = 2.4$. (C) Period for $m = 3$. (D) Period for $m = 4$

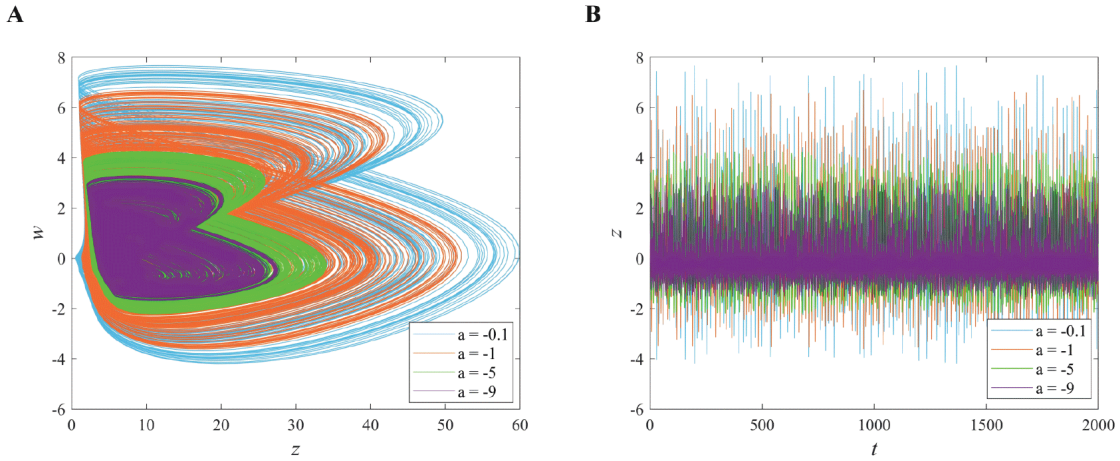

Figure 7. Chaotic amplitude modulation of the memristive chaotic system with $b = 3,\ c = 1.5,\ d = 0.1,\ e = 1,\ m = 2,\ n = 0.2$ and variation of a. (A) Corresponding phase projection on $z - w$. (B) Time series of z

global coordinates. **Figure 10** shows the symmetric chaotic attractor pairs generated within the $(x,\ w)$ and $(z,\ w)$ planes when the initial values are $[-1,\ 1,\ 1,\ 1]$, $a = -1$, $b = 3$, $c = 1.5$, $d = 0.1$, $m = 2$, $n = 0.2$, and $e = \pm 1$.

In summary, the amplitude modulation exhibited by the NE_2-MCS has important engineering value. It can autonomously generate flexible and adjustable chaotic signals without relying on external control methods or additional devices, substantially improving the system's applicability across various chaos-based applications and meeting diverse requirements in different scenarios. At the same time, the NE_2-MCS exhibits rich signal-control characteristics, such as signal amplitude modulation

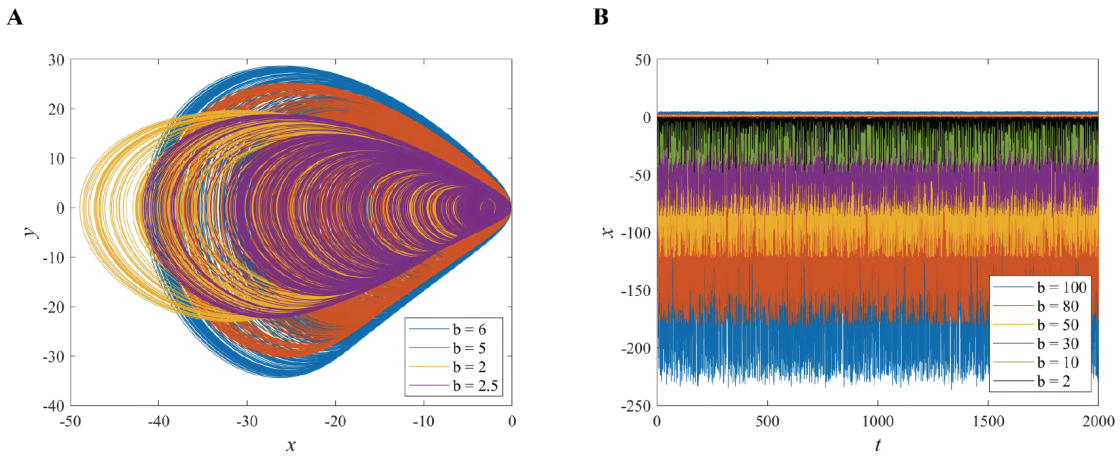

Figure 8. Chaotic amplitude modulation of the memristive chaotic system with $a = 1$, $c = 1.1$, $d = 0.2$, $e = 1$, $m = 2$, $n = 0.2$, and variation of b. (A) Corresponding phase projection on $x - y$. (B) Time series of x

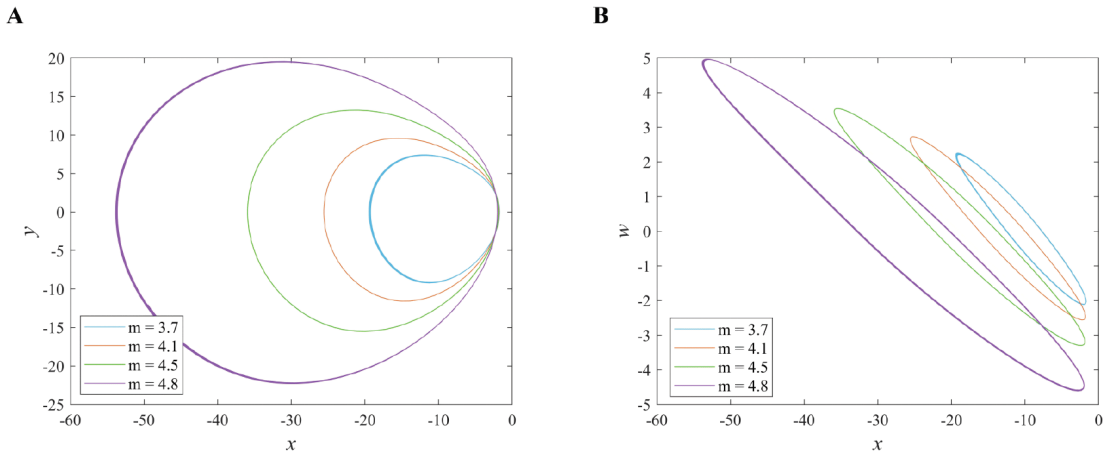

Figure 9. Periodic amplitude modulation of the memristive chaotic system with $a = 1$, $b = 2$, $c = 1.1$, $d = 0.2$, $e = 1$, $n = 0.2$, and variation of m. (A) Corresponding phase projection on $x - y$. (B) Corresponding phase projection on $x - w$

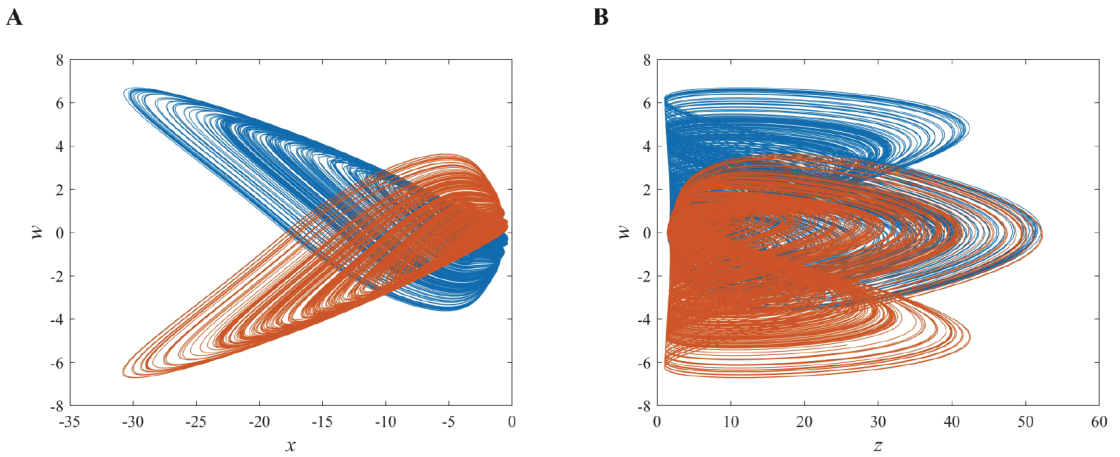

Figure 10. Partial mirror symmetry of the memristive chaotic system with $a = -1$, $b = 3$, $c = 1.5$, $d = 0.1$, $m = 2$, $n = 0.2$, and $e = \pm 1$ ($e = 1$ is red, $e = -1$ is blue). (A) Corresponding phase projection on $x - w$. (B) Corresponding phase projection on $x - z$

across different scales. This provides an effective technical approach for achieving high-precision signal modulation, designing chaotic signal sources with adjustable dynamic ranges, and controlling complex systems. Moreover, benefiting from the partial mirror symmetry mechanism, the NE_2-MCS can produce symmetric dynamical behaviors. In practical engineering implementations, chaotic signals with adjustable amplitude and polarity can be conveniently realized by tuning the intrinsic structural parameters of the system, thereby further enhancing the operational flexibility

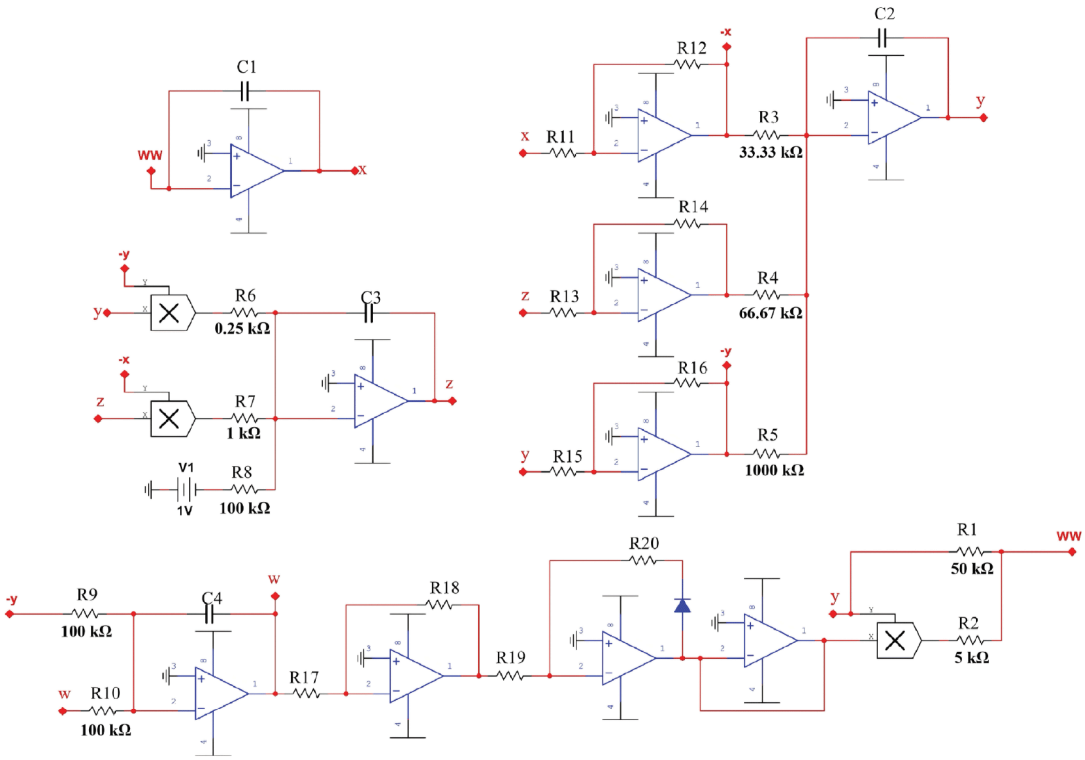

Figure 11. Circuit diagram of a memristive chaotic system

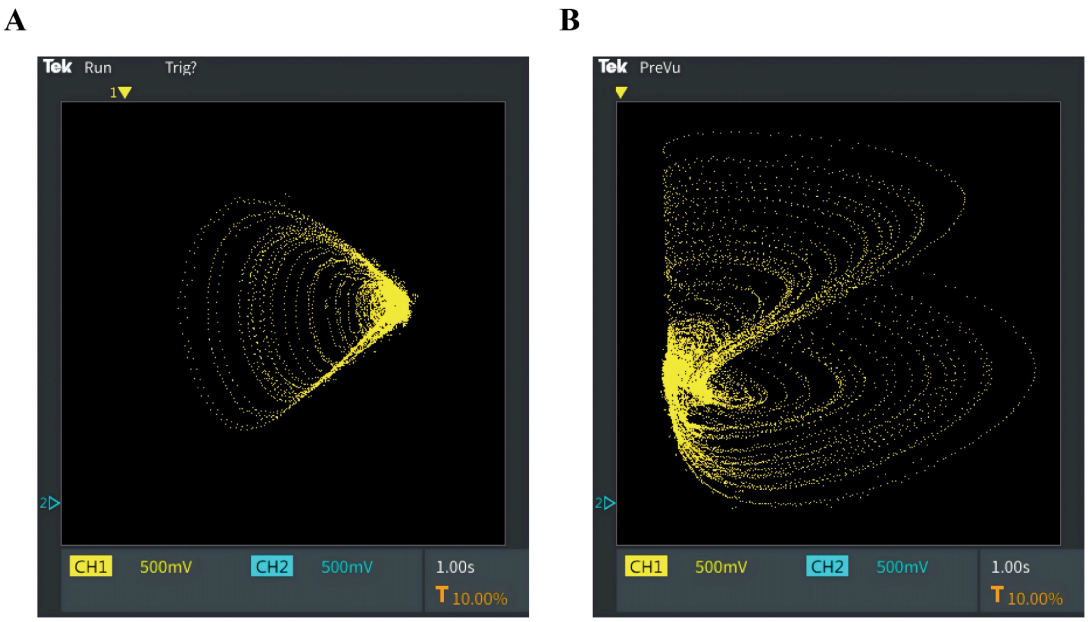

Figure 12. Experimental circuit results of the memristive chaotic system. (A) $x - y$. (B) $z - w$

and engineering potential of the presented memristive chaotic oscillator.

4. Circuit implementation

The circuit implementation of chaotic systems holds substantial practical significance, as it not only substantiates the physical realizability of the system's dynamical behaviors but also facilitates the generation of pseudo-random chaotic signals suitable for real-world applications. An oscilloscope, as a typical experimental measurement instrument, provides reliable and intuitive waveform observation, thereby effectively verifying the consistency between theoretical analysis and actual hardware performance. Accordingly, it is widely adopted in the hardware realization of chaotic systems. In this section, an oscilloscope is used to test and verify the NE_2-MCS circuit implementation to confirm its physical feasibility.

The system's variables exceeded the op-amp's dynamic range. To solve this problem, we applied uniform

compression and adjusted the time scale. Let τ=τ_0t, where τ_0= 100, the scaled state equation is given as follows:

$$\begin{cases} \dot{x} = -100my - 1000n|w|y \\ \dot{y} = 100bx + 100cz + 100ky \\ \dot{z} = 4000y^2 + 1000xz - 100a \\ \dot{w} = 100dy - 100w \end{cases} \tag{8}$$

Based on **Equation 8**, an analog circuit is designed to implement the dynamical behavior described by the four-dimensional differential equations. The differentiation operations in the system are converted into op-amp integrator circuits through the relationship $\dot{w} \leftrightarrow \int w\ dt$. Multiplicative terms such as y^2, xz, and $|w|y$ are implemented using analog multipliers. Proportional coefficients, including 100, 1,000, and 4,000, are matched through resistor voltage-divider or proportional amplifier configurations. Constant terms such as $-100a$ are introduced by superimposing direct current voltage sources. Through these implementations, the complete four-dimensional differential system is realized in an analog circuit, enabling physical verification of its dynamic characteristics via oscilloscope measurements. When we set the parameters to $a = -1$, $b = 3$, $c = 1.5$, $d = 0.1$, $e = 1$, $m = 2$, $n = 0.2$, the circuit shown in **Figure 11** can be transformed into a set of circuit equations (**Equation 9**):

$$\begin{cases} \dot{x} = -\frac{1}{R_1C_1}y - \frac{1}{10R_2C_1}|w|y \\ \dot{y} = -\frac{1}{R_3C_2}(-x) - \frac{1}{R_4C_2}(-z) - \frac{1}{R_5C_2}(-y) \\ \dot{z} = -\frac{1}{10R_6C_3}(-y^2) - \frac{1}{10R_7C_3}(-x)z - \frac{1}{R_8C_3} \\ \dot{w} = -\frac{1}{R_9C_4}(-y) - \frac{1}{R_{10}C_4}w \end{cases} \tag{9}$$

Let $C_1 = C_2 = C_3 = C_4 = 100$ nF, $R_{11-20} = 10$ kΩ. By comparing **Equations 8 and 9**, we can obtain R_1= 50 kΩ, R_2= 5 kΩ, R_3=33.33 kΩ, R_4= 66.67 kΩ, R_5= 1000 kΩ, R_6= 0.25 kΩ, R_7= 1 kΩ, $R_8 = R_9 = R_{10} = 100$ kΩ. The initial voltages are set to $[-0.01,\ 0.01,\ 0.01,\ 0.01]$. **Figure 12** shows the results captured by the oscilloscope, corresponding to the projections of the system on the $x - y$ plane and $z - w$ plane, respectively. The figure shows that the theoretical analysis is consistent with the numerical simulation results, thereby verifying the existence of the NE_2-MCS to a certain extent.

5. Conclusion

The current study constructs a novel four-dimensional NE_2-MCS with rich dynamic characteristics by introducing a non-ideal absolute-value memristor to expand the dimensionality of a classical three-dimensional chaotic system. It can flexibly switch between equilibrium points and without equilibrium points via key parameter adjustment, exhibiting diverse parameter-dependent bifurcation dynamics. Notably, the proposed system exhibits core characteristics, including multi-parameter amplitude modulation, large-scale amplitude modulation, and partial mirror symmetry, yielding chaotic output signals with excellent controllability and morphological diversity. This study provides a new method and core technical support for the design of chaotic signal sources in engineering applications such as secure communication and image encryption, effectively addressing the deficiencies of existing chaotic systems in flexible dynamic characteristics and equilibrium point manipulation. To verify physical realizability, we present oscilloscope measurements of the corresponding memristive chaotic circuit, and the experimental results are highly consistent with the theoretical analysis, thereby confirming the engineering feasibility of the system. This study not only enriches the construction methods and dynamic analysis system of MCS but also provides new theoretical perspectives and experimental evidence for nonlinear signal processing, memristive circuit design, and other fields, demonstrating important academic value and application potential.

The current study provides a basis for in-depth research and engineering application of MCS with switchable equilibrium points, and multiple research directions with important academic value and application potential await further exploration and expansion. First, the memristor embedding method proposed in this paper can be extended to classical chaotic systems, such as Lorenz and Chen systems, to explore the universality of equilibrium-switching and multi-parameter amplitude modulation mechanisms, thereby establishing a general construction framework for high-dynamic MCS and enriching the family of MCS with complex dynamics. Second, the fractional-order extension of the proposed NE_2-MCS is of great research significance, and systematic analysis on the fractional-order form can explore the influence of fractional-order parameters on the system's equilibrium switching, bifurcation evolution, and amplitude modulation, which will further exploit the dynamic potential of the system and enhance the complexity of chaotic signals to better meet the requirements of high-security engineering applications. Third, based on existing circuit simulations and actual measurement verification, further research on the hardware implementation of the system on field-programmable gate arrays, embedded platforms, and other practical hardware can be conducted, combined with performance evaluation from the perspectives of power consumption, real-time performance, and anti-interference capability. In addition, in-depth research on active control strategies for chaotic states, amplitude modulation and symmetry of the system, and the improvement of synchronization control schemes for secure communication scenarios will provide more comprehensive technical support for the practical deployment of the system in resource-constrained edge devices and its wide application in the field of nonlinear signal processing.

Acknowledgments

None.

Funding

None.

Conflict of interest

The author declares no conflicts of interest.

Author contributions

This is a single-authored article.

Availability of data

Not applicable.

AI tools statement

The author confirmed that no AI tools were used in the preparation of this manuscript.

References

1. Lai, Q, Zhu, CK, Zhao, XW, Sun, X, Hua, JL, & Hua, JL. A unified framework for generating 4D discrete memristive hyperchaotic maps with complex dynamics and application to encryption. *IEEE Internet of Things J*. 2025; 12(19):40934-40943. https://doi.org/10.1109/jiot.2025.3590465
2. Wang, L, Song, W, Di, J, Zhang, X, Zou, C. Image Encryption Method Based on Three-Dimensional Chaotic Systems and V-Shaped Scrambling. *Entropy*. 2025; 27(1):84. https://doi.org/10.3390/e27010084
3. Zhao, Z, Yang, R, Liu, J, Liu, G. Study on weak signal amplitude detection and circuit simulation based on a new chaotic system. *Chaos, Solitons & Fractals*. 2025; 198: 116554. https://doi.org/10.1016/j.chaos.2025.116554
4. Pan, G, Li, C, Liu, W, Xue, Y, Qi, X. Countless coexisting chaotic attractors: From system construction to FPGA-based observation. *Chaos, Sol & Frac*. 2025; 198: 116610. https://doi.org/10.1016/j.chaos.2025.116610
5. Jie, J, Yang, Y, Zhang, P. The construction method of chaotic system model based on state variables and uncertain variables and its application in image encryption. *Appl Math Model*. 2025; 144: 116097. https://doi.org/10.1016/j.apm.2025.116097
6. Erkan, U, Toktas, A, Toktas, F, Lin, YT, Gao, S. Hybridization of benchmark functions for a high-performance 1D chaotic map and image encryption application. *Non lSci and Cont Eng*. 2025; 1(2):025340010. https://doi.org/10.36922/NSCE025340010
7. Yang, H, Liu, Y, Li, G. Analysis of 3D chaotic system with novel double scroll structure and additional nonlinear functions and its application in weak signal detection. *Eur Phys J Plus*. 2025; 140(7):637. https://doi.org/10.1140/epjp/s13360-025-06542-3
8. Li, D, Chen, Z, Yin, FL. A robust and secure audio zero-watermarking scheme based on novel chaotic map and dual-tree complex wavelet transform. *IEEE Internet of Things J*. 2025; 12(15), 29614-29625. https://doi.org/10.1109/JIOT.2025.3569457
9. Zaamoune, F, Tinedert, IE, Menacer, T. Analysis of novel 3D chaotic system, hidden coexisting, adaptive control, offset boosting control, and circuit implementation. *Eur J Control*. 2025; 84: 101259. https://doi.org/10.1016/j.ejcon.2025.101259
10. Zhou, K, Zhang, J, Xiang, J, Zhong, Y. Multi-image encryption combining four-dimensional chaotic systems and multi-layer embedding. *Eur Phys J Spec Top*. 2025; 234(9):2827-2844. https://doi.org/10.1140/epjs/s11734-024-01321-0
11. Bell, S, Cookson, TJ, Cope, SA, *et al*. Experience with variable-frequency drives and motor bearing reliability. *IEEE Trans Ind Appl*. 2001; 37(5):1438-1446. https://doi.org/10.1109/28.952519
12. Lai, Q, Qin, MH. Universal method for enhancing dynamics in neural networks via memristor and application in IoT-based robot navigation. *IEEE Trans Cybern*. 2026; 56(1):557-566. https://doi.org/10.1109/TCYB.2025.3607140
13. Khan, A, Li, C, Zhang, X, Cen, X. A two-memristor-based chaotic system with symmetric bifurcation and multistability. *Chaos and Frac*. 2025; 2(1):1-7 https://doi.org/10.69882/adba.chf.2025011.
14. Fan, S, Xu, X, Liu, X, Cao, Y, Gao, S, Mou, J. Complex neuronal dynamics under memristive electromagnetic radiation: Modeling and digital signal processing implementation. *Non Sci and Cont Eng*. 2025; 1(2):025400013 https://doi.org/10.36922/NSCE025400013
15. Yan, S, Wang, J, Zhang, J. Analysis and application of discrete 3D no equilibrium points memristive Hindmarsh-Rose models. *Eur Phys J Spec Top*. 2025; 1-18. https://doi.org/10.1140/epjs/s11734-025-01665-1
16. Fan, C, Ding, Q. Design and dynamic analysis of a class of new 3-D discrete memristive hyperchaotic maps with multi-type hidden attractors. *Chaos, Sol & Frac*. 2025; 191: 115905. https://doi.org/10.1016/j.chaos.2024.115905
17. He, SQ, Yu, F, Guo, R, *et al*. Dynamic analysis and FPGA implementation of a fractional-order memristive Hopfield neural network with hidden chaotic dual-wing attractors. *Frac & Frac*. 2025; 9(9):561. https://doi.org/10.3390/fractalfract9090561
18. Kalaichelvi, K, Rameshbabu, R, Priya, VD, Rithanya, PG, Bhavadharani, GK, Gayathiri, KS. A Novel Chaotic Jerk System with Multistability and Its Circuit Implementation. *Non Dy & Sys The*. 2025; 25(2):220. https://e-ndst.kiev.ua/v25n2/5(98).pdf
19. Rahman, ZASA, Jasim, BH, Al-Yasir, YIA, Abd-Alhameed, RA. High-security image encryption based on a novel simple fractional-order memristive chaotic system with a single unstable equilibrium point. *Elec*. 2021; 10(24):3130. https://doi.org/10.3390/electronics10243130
20. Yu, F, Tan, B, He, T, *et al*. A wide-range adjustable conservative memristive hyperchaotic system with transient quasi-periodic characteristics and encryption application. *Math*. 2025; 13(5):726. https://doi.org/10.3390/math13050726
21. Wang, QM, Wang, L, Wen, W, Li, Y, Zhang, G. Dynamical analysis and preassigned-time intermittent control of memristive chaotic system via T–S fuzzy method. *Chaos: An Interdisciplinary Journal of Nonlinear Science*. 2025; 35(2). https://doi.org/10.1063/5.0221159
22. Wan, ZQ, Pu, YF, Lai, Q. Memristive feedback-controlled chaotic system with diverse dynamics. *Non Sci & Cont Eng*. 2025; 1(1):025310008. https://doi.org/10.36922/NSCE025310008
23. Feng, XY, Lu, TA, Zhou, L. A 4D memristive chaotic system with multiple amplitude and offset controllers. *Phy Scri*. 2025; 100(6):065237. https://doi.org/10.1088/1402-4896/add844
24. Wang, YC, Zhang, S, Wang, Z, Wang, J, Peng, X, Hua, G. Robust Enhanced Chaos in Memristive Multi-attractor Rulkov Neuron Model with Application to Hardware Image Cryptosystem. *IEEE Internet of Things J*. 2025; 12(15):32022-32034. https://doi.org/10.1109/jiot.2025.3575569
25. Zhang, S, He, D, Li, Y, Lu, D, Li, C. Dual Memristor-coupled Hopfield Neural Network with Any Multi-scroll Amplitude Control and Its Application for Medical Image Classification. *IEEE Trans Autom Sci Eng*. 2025; 22: 17828-17840. https://doi.org/10.1109/TASE.2025.3585935
26. Lai, Q, Liu, YJ, Liu, F, Zhao, XW. Generating grid multiscroll memristive Chua's circuit and its predefined-time synchronization for secure communication. *IEEE Transactions on Circuits and Systems I: Regular Papers*. 2025; 72(10):5947-5956. https://doi.org/10.1109/TCSI.2025.3541635
27. Lin, YT, Liao, YL, Wei, YN, *et al*. Lightweight image encryption via four-dimensional Hénon memristor map and fast block permutation. *Non Sci & Cont Eng*. 2025; 1(2):025390012. https://doi.org/10.36922/NSCE025390012